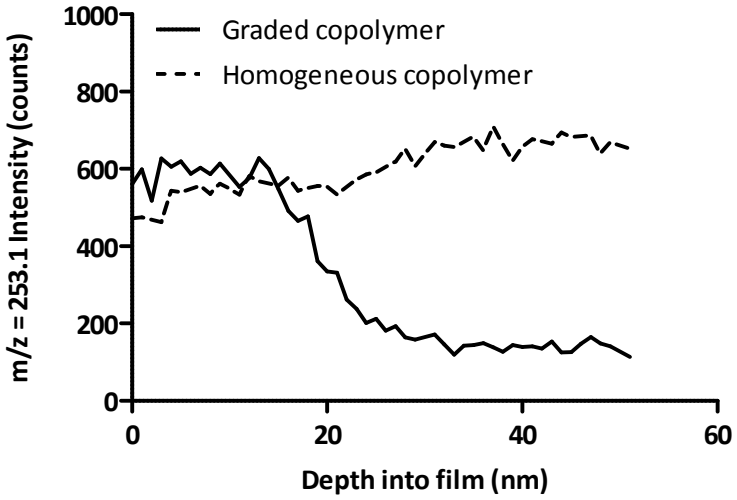

Figure 2.5. ToF-SIMS depth profile of GP and HP.
Showing signal from m/z = 253.1, corresponding to a positively charged PFM fragment, as a function of film depth for both the bulk and graded co-polymer (samples H and G, respectively).

2.3.3. Hydrogel Swelling Properties and Thin Film Structure

Thin films used as protective overlayers for biosensors must allow for the passage of small analytes from the medium to the sensor. It is therefore critical that the film swell when in contact with a biological medium while remaining adhered to the sensor substrate. All the films synthesized in this study exhibited a rapid and reversible swelling response, while maintaining excellent film adherence to the substrate. As characterized by *in situ* spectroscopic ellipsometry, the films reached their equilibrium swollen water content within 5 min of incubation in buffer solution. Upon rinsing in deionized water and drying under vacuum, the films returned to their original thickness. When incubated again, the films rapidly returned to their swollen state. Figure 2.6. shows a typical response to several of these swell/dry cycles. Despite the fact that the piCVD films are simply physisorbed to the silicon substrate and not

covalently bound, the original thickness is recovered after each swell/dry cycle. This suggests that polymer does not leach out of the film, when incubated in buffer solution, demonstrating its potential for biological or physiological applications. This behavior also indicates that the cross-linking within the film is not exclusively due to physical entanglements; since physical cross-linking alone would result in the loss of film in the swelling and washing steps. The swollen water content is the volume fraction of water in the film when swollen in aqueous phosphate buffer solution.

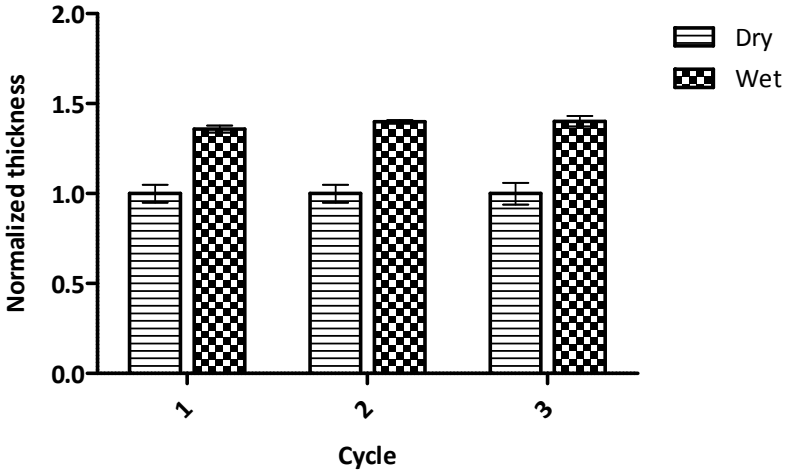

Figure 2.6. Typical reversible swelling response of piCVD pHEMA.
For multiple swell/dry cycles in PBS buffer solution (pH 7.4). All thicknesses are normalized to the as-deposited thickness of 200 nm.

To control the swellability of these films, it is important to understand, whether the polymerization is initiated in the vapor phase or on the substrate surface. Figure 2.7. shows the swellability as a function of vapor residence time in the reactor (experimental series A). The residence time was determined by dividing the chamber volume (5467 mL) by the vapor flow-rate. Changing the residence time alters UV exposure time for gaseous monomer

molecules as they pass through the reactor. Results showed that changes in the residence time did not have a notable effect on film swellability. The relative independence of film swellability on irradiation time suggests that the polymerization is not a vapor phase process and that irradiation chemistry at the surface is the dominant initiation mechanism for film deposition.

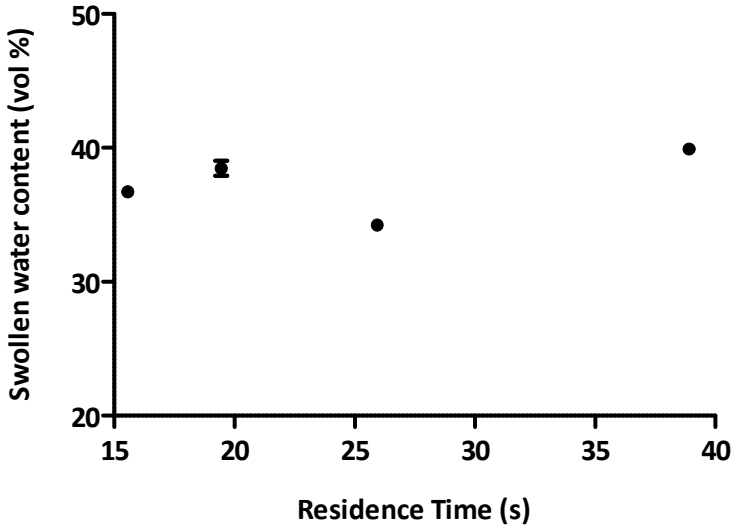

Figure 2.7. Swollen water content as a functional of vapor residence time.

In order to prove that the initiation mechanism is a surface phenomenon, the surface concentration of monomer was systematically varied, while the residence time was maintained constant throughout the experiment (experimental series B). This was accomplished by varying the ratio of the partial pressure of the monomer to its saturation pressure at the stage temperature, P_M/P_M^{sat}. This ratio will be referred to as the fractional saturation of the monomer and has previously been shown to control the concentration of monomer on the substrate (Lau & Gleason 2006). The saturation pressure is evaluated using the Clapeyron equation. Figure 2.8 indicates a strong dependence of P_M/P_M^{sat} on film swellability, which indicates that the polymerization takes place at the surface. Changing

P_M/P_M^{sat}, and therefore, a change in the P_M/P_M^{sat} – i.e. the surface concentration of monomer – during the synthesis allows for the careful control of the swelling properties of the resulting film.

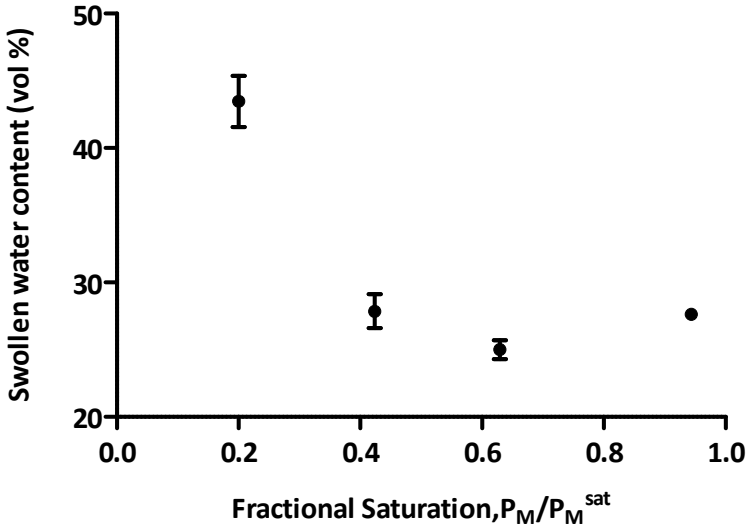

Figure 2.8. Equilibrium swollen water content as a functional of fractional saturation of monomer during deposition.
Each measurement was performed three times on the same sample, and the error bars indicate the standard deviation of the measurements.

The moderate degree of swelling and the reversibility of the swelling response suggest that the films are highly cross-linked. The origin of the cross-linking is unclear because no cross-linking agents were introduced into the reactor. However, if the pendant carbonyl group can be decomposed into radicals under UV irradiation, as suggested earlier, then each pendant group on the polymer chain can potentially act as a cross-linker. Furthermore, HEMA monomer may undergo transesterification or etherification leading to dimethacrylates, which are commonly used as cross-linking agents (J. Lee et al. 2002; Vasilopoulou et al. 2004). Finally, physical cross-linking via chain entanglement may not be fully discarded, although purely physical cross-

linking is unlikely given the stability of the film over several swell/dry cycles. Understanding the degree of cross-linking, regardless of the chemical nature of the cross-links, is critical to understand how these films can potentially be used to determine the potential of these films as protective layers for sensors in biological environments. Non-specific protein adhesion can potentially damage devices, thus the film must be cross-linked enough to prevent passage of proteins from the biological medium to the device surface. At the same time, analytes must be able to permeate across the film to reach the sensing device.

As shown before, the cross-linking of the film is intimately related to the swollen water content of the film. In order to assess other parameters that may affect the water-swelling ability of the films, films of different thicknesses were subjected to buffer incubation and their swollen water content was determined. Figure 2.9. shows the swellability as a function of deposited thickness (experimental series C). It was noticed that the swollen water content is limited by the hydrogel thickness, since thicker films are able to absorb water to a lesser extent.

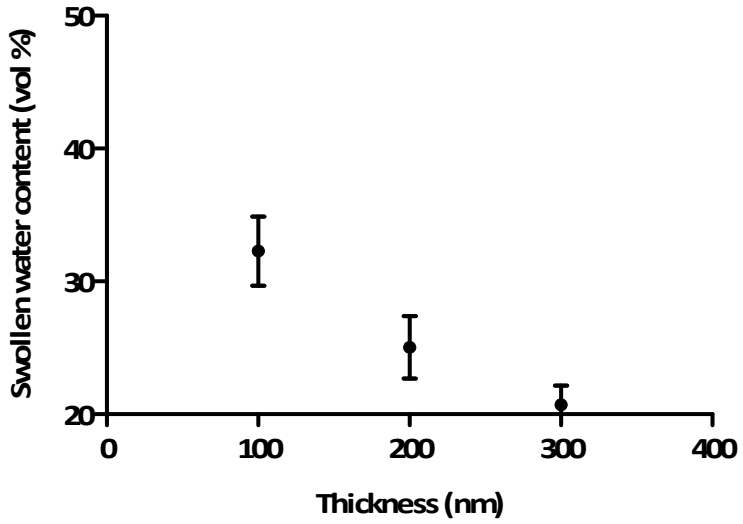

Figure 2.9. Equilibrium swollen water content as a function of deposited thickness

Another parameter that has been study to evaluate its influence in the swelling ability of the films was the distance between the sample and the UV lamp. Figure 2.10. shows the dependence of swollen water content on distance between the sample and the UV lamp (experimental series D). The UV light intensity coming in contact with the sample varies depending on the light-sample gap. At each distance, deposition rate increases significantly with increasing the gap, but no discernible trend in the mechanical properties can be made.

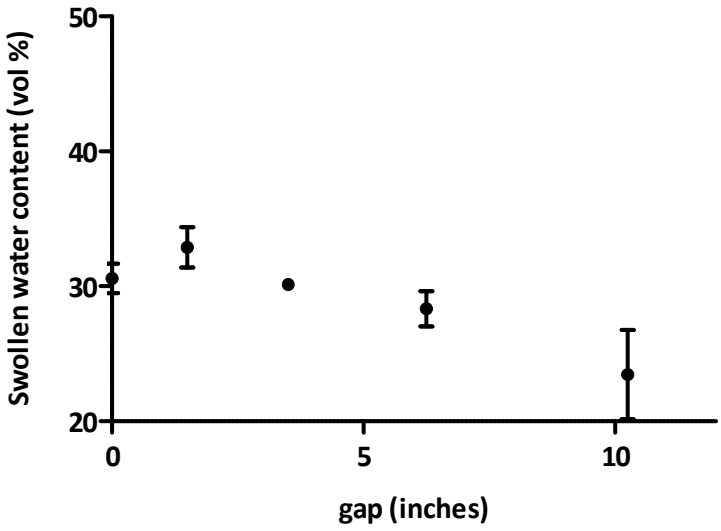

Figure 2.10. Equilibrium swollen water content as a functional of distance between the sample and the UV lamp.

As discussed earlier, the ability to swell defines the nature and function of a hydrogel. Consequently, conservation of swelling properties while incorporating the surface-active components is extremely important. In order to evaluate the swelling behavior of bulk vs. graded co-polymers, both types of films were deposited on silicon wafers, incubated in buffer solution and their swelling capacity was determined by ellipsometry Figure 2.11. shows the

swollen water content for the bulk and graded co-polymers at different HEMA/PFM monomer ratios. It can be observed that with an increasing PFM content, the swollen water content decreases from 25% (pure pHEMA) to 3% (71% PFM). The bulk co-polymer does not retain the swelling properties of HEMA due to the hydrophobicity of PFM. However, for the graded co-polymers, the swollen water content of pure pHEMA is notably retained even with increasing PFM content. These results suggest that the physical swelling properties of a hydrogel can largely be maintained even after incorporating an ultrathin co-polymeric layer. This allows the selection of the underlying physical properties of the hydrogel independently from the chemical properties of the surface activity.

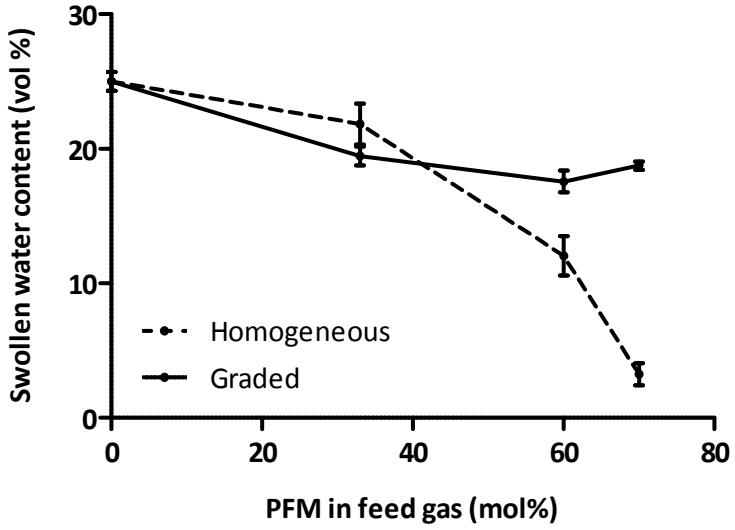

Figure 2.11. Swollen water content as a function of the increasing PFM content for both the bulk and graded co-polymer.

The cross-linking is intimately related to the swollen water content of the film; for highly cross-linked networks, the swollen water content and the average molecular weight between cross-links satisfy the following equation (Lucht & Peppas 1981).

$$\frac{1}{M_C} = \frac{2}{M_n} - \frac{\frac{\bar{v}}{V_1} \times \left[ln(1 - v_{2,s}) + v_{2,s} + X(v_{2,s})^2\right]\left[1 - \frac{M_r}{2\bar{M}_C}(v_{2,s})^{1/3}\right]^3}{\left((v_{2,s})^{1/3} - \frac{1}{2}v_{2,s}\right)\left(1 + \frac{M_r}{2\bar{M}_C}(v_{2,s})^{2/3}\right)^2}$$

Equation 2.1.

Where $\bar{M}_C$ is the average molecular weight between cross-links, $\bar{v}$ is the specific volume of pHEMA (0.87 $cm^3 \cdot g^{-1}$), V_1 is the molar volume of water (18 $cm^3 \cdot mol^{-1}$), M_r is the molecular weight of the HEMA repeat unit (130 $g \cdot mol^{-1}$), $v_{2,s}$ is the ratio of the thickness of the dry polymer to the thickness of the swollen polymer (measured via ellipsometry), and X is the Flory-Huggins interaction parameter (varies with water content (Janacek & Hassa 1966)).

This theory was developed for linear polymer chains of number average molecular weight $\bar{M}_n$ that undergo cross-linking by the introduction of a cross-linking agent. Measuring $\bar{M}_n$ for the piCVD films is difficult because the cross-linking occurs *in situ* and without a separate chemical agent. Here, $\bar{M}_n$ is assumed to be large enough so that the term in which it appears can be neglected. The molecular weight between cross-links can in turn be used to evaluate the average mesh size in the swollen film (Peppas et al. 1985; Canal & Peppas 1989). It should be noted that the cross-link density as calculated by Equation 2.1, is an effective value that does not distinguish between physical entanglements and chemical cross-linking. The most likely source of uncertainty in this calculation lies in the measurement of the swollen water content and, therefore, $v_{2,s}$. Figure 2.12. shows the average mesh size for films B1 - B4 as obtained by Equation 2.1., including the propagated uncertainty in $v_{2,s}$. Each of these mesh sizes is larger than the hydrodynamic radii of physiologically relevant analytes. For example, sugars, such as glucose and sucrose, and metal cations, such as Na^+ and Mg^{2+} have hydrodynamic radii below than 0.5 nm (Schultz & Solomon 1961; Pappenheimer et al. 1951; Hussain et al. 2008) and

should easily permeate the mesh. However, these mesh sizes are small enough to avoid permeation of larger biomolecules, such as proteins. For example, albumin is a 3.8 x 15.0 nm ellipsoid molecule and fibrinogen is a 9 x 45 nm ellipsoid (Werner et al. 1999).

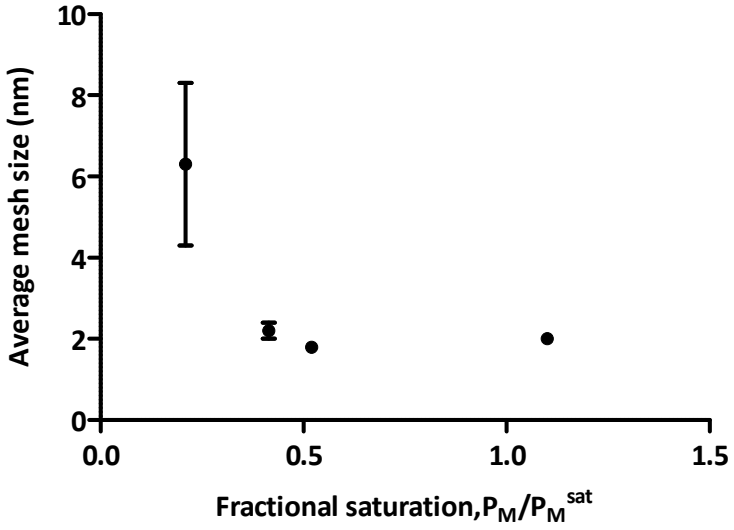

Figure 2.12. Average mesh size of swollen films, as calculated by Equation 2.1.
The error bars indicate the uncertainty resulting from propagating the error of the corresponding swollen water content measurement in Figure 2.8.

2.3.4. Protein Adhesion on pHEMA Surface

In order to check the feasibility of hydrogel film formation on the surface of sensor devices as protection strategies against protein adhesion, the non-specific adhesion on piCVD-deposited films was determined. While the films are capable of protecting device surfaces from contact with proteins, the films themselves should also resist non-specific protein adhesion. XPS characterization of the piCVD films following incubation in a protein solution provided a convenient technique for measuring the degree of protein adhesion. Briefly, triplicates of B2 samples and bare silicon wafers were incubated in a bovine serum albumin solution for three

hours at 37 ^{o}C. Samples were then rinsed with PBS buffer solution to remove any unbound protein, dried gently under nitrogen and XPS analysis was performed to quantify the degree of non-specific protein adhesion on both pHEMA films and bare silicon.

Since the pHEMA films do not contain nitrogen, nitrogen detection by the highly surface-sensitive XPS technique shall correlate with the presence of surface-bound proteins must be due to the presence of surface-bound proteins. Figure 2.13. compares the nitrogen content of a pHEMA surface incubated in a solution of BSA against a control silicon surface. The HEMA film exhibits an 8-fold decrease in surface nitrogen signal over bare silicon, which can only be attributed to a reduction of surface-bound proteins.

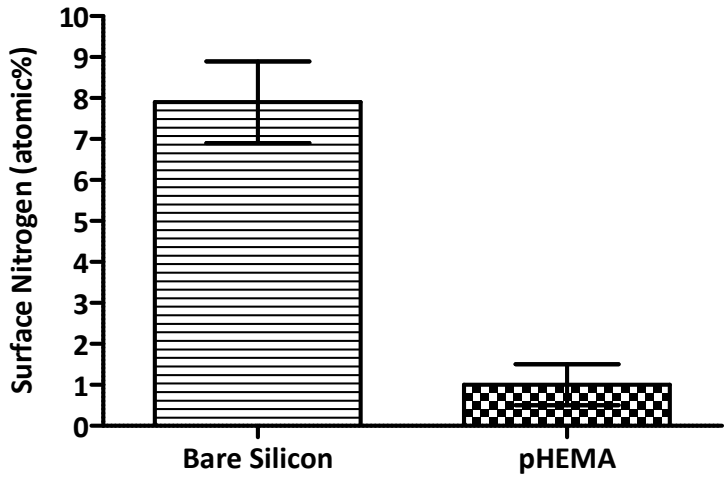

Figure 2.13. Surface nitrogen content.
Content after incubation in a 1% w/v bovine serum albumin solution for three hours at 37 ^{o}C.

2.3.5. pHEMA-based Hydrogel Functionalization

The pentafluorophenyl ester moiety used to functionalize the polymer surface is known to react rapidly with amine groups. During the reaction, the pentafluorophenyl group is replaced by an amide bond (Francesch et al. 2007). This reactivity allows the functionalization of the hydrogel by any nucleophilic agent in a single-step reaction. In order to evaluate the reactivity of HEMA/PFM co-polymer films, both bulk and graded films were allowed to react with an amine-bearing reagent and changes in their chemical composition were followed by infrared spectroscopy. Figure II.XIIIa and figure II.XIIIb show the spectra before and after incubation/reaction with PEG-diamine of bulk and graded co-polymers, respectively.

After functionalization, a strong and wide band is expected to appear at 1107 cm^{-1}, attributed to the C-O vibration of the PEG. In both the functionalized bulk and graded co-polymers, PEG functionalization is confirmed by the presence of this band in the FTIR spectra. There is far more PFM in the bulk co-polymer so, as expected, there is far more PEG attached to the bulk co-polymer. As expected, IR shows a higher amount of PEG attached to bulk co-polymer films, due to the higher concentration of PFM groups in these co-polymers. However, the absorption signals corresponding to the fluorinated phenyl ring disappear completely only in the case of the graded co-polymer. This suggests that the functionalized bulk co-polymer contains a significant fraction of unreacted PFM that can be susceptible of undesired subsequent reactions with nucleophiles. Unlike the bulk co-polymers, the graded co-polymer allows a complete conversion of the reactive PFM groups.

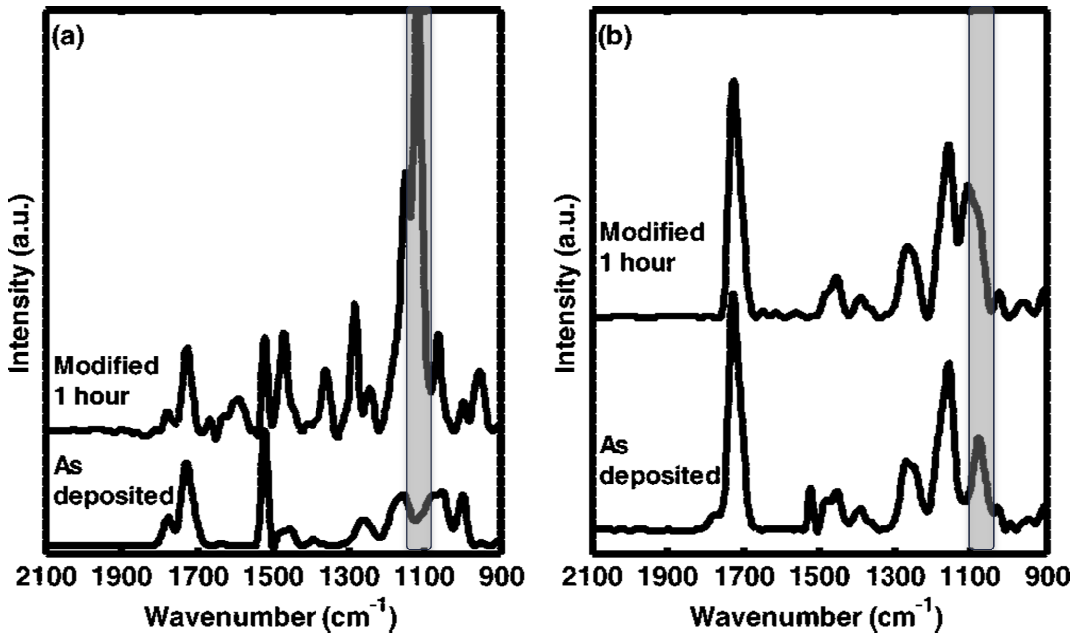

Figure 2.14. FTIR spectra of the co-polymer synthesized by piCVD before and after the functionalization with H_2N-PEG-NH_2.

(a) Bulk co-polymer (sample H3); (b) graded co-polymer (sample G3).

This phenomenon could be explained due to difficulty of the reactive amines to diffuse through the film, localizing the reaction on the first nanometers of the hydrogel surface. This could be especially important, when the films would be functionalized with large biomacromolecules, such as proteins.

2.3.6. Silica Microspheres and Sensor Coated with pHEMA Thin Film

To demonstrate the gentle nature of the piCVD process, a sodium-sensing optode was coated with a 100 nm film of pHEMA. The optode is a chromoionophore and an ionophore casted as a film (<10 μm thickness) in a polymer matrix on a 10 mm diameter glass coverslip. In order to evaluate the influence of the hydrogel-film coating on the optode surface, a functional experiment to compare the sensor response was performed on uncoated and coated optodes.

The responses of both an uncoated optode and a coated optode to varying levels of sodium ion concentration are shown in Figure 2.15.

Results show identical sodium response signals for both coated and uncoated sensors. In addition, the coated optode shows equivalent response times, when compared to the uncoated optode. Therefore, the piCVD process surface treatment does not seem to damage the optode functionality. Since the response of the device is governed by the diffusion of sodium ion through the optode matrix, which is several microns thick (Shortreed et al. 1996), results indicate that ion diffusion is not affected by the presence of the hydrogel thin film

The nanoscale thickness of the overlaying pHEMA film does not add significantly affect to the distance that the ion must diffuse. Additionally, the fact that the sodium ion diffuses through the film is consistent with the calculated mesh size. Small molecule analytes, such as ions, have no difficulty diffusing through a film with a mesh size in the order of several nanometers.

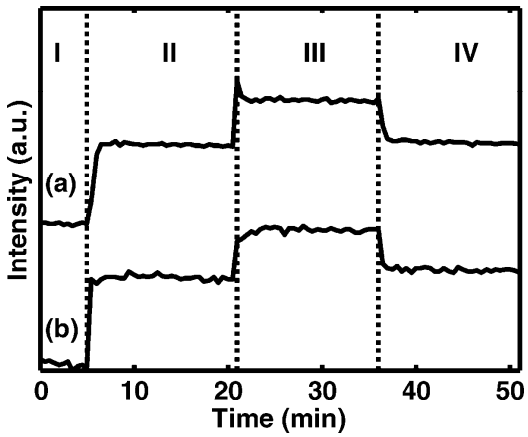

Figure 2.15. Response curves of an uncoated and coated optodes.
(a) uncoated optode and (b) optode coated with 100 nm piCVD pHEMA. The intensity is the fluorescence emission ratio of 570/670 nm, after excitation at 485 nm. The curves show the response of the optodes, when incubated in phosphate buffer at pH 7.4 containing NaCl at I, 0 Na^+; II, 140 mM Na^+; III, 340 mM Na^+; and IV, 140 mM Na^+

Since piCVD is a dry process, the geometries that can be coated with pHEMA are not limited to planar surfaces. Indeed, many sensors of physiologically relevant analytes are being miniaturized as microparticles to take advantage of high surface areas and decreased response times (Shortreed et al. 1996; Zhou et al. 2005). As a dry process, piCVD can conformally coat microgeometries, while avoiding the effects of solvent surface tension, which may induce particle agglomeration. In order to check the potential of such techniques to conformationally coat microgeometries, defined microparticles were subjected to piCVD. Figure 2.16. shows a cross section of a ~50 μm microsphere coated with approximately 1 μm of pHEMA. It can be observed that the coating is continuous and conformal around the outside of the particle.

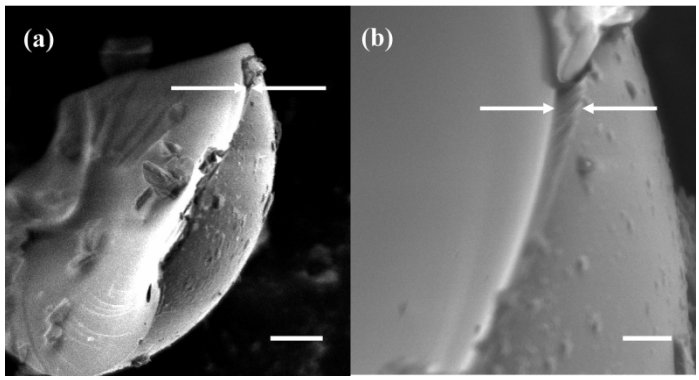

Figure 2.16. SEM cross-section of a 50 μm silica microsphere coated with piCVD pHEMA.
At (a) 1600× magnification (scale bar = 10 μm) and (b) 5500× magnification (scale bar = 2 μm). The arrows indicate the polymer layer

The same experiment was repeated on particles having a smaller diameter to challenge the technique. Figure 2.17. shows SEM images of uncoated and coated monodisperse microparticles that were placed in a wafer with no shaking method applied (see 2.2.3) and were coated in a single piCVD run. The uncoated microspheres had an average diameter of 5.06 ± 0.04 μm and the coated microspheres had an average diameter of 5.39 ± 0.04 μm,

indicating that the particles were coated with approximately 165 nm of hydrogel. The same method was used to coat smaller particles having a diameter of approximately 800 nm. AFM imaging shows the average diameter of the uncoated and coated spheres (Figure 2.18.). The difference indicates a diameter increase of 400 nm, 200 nm per microsphere side.

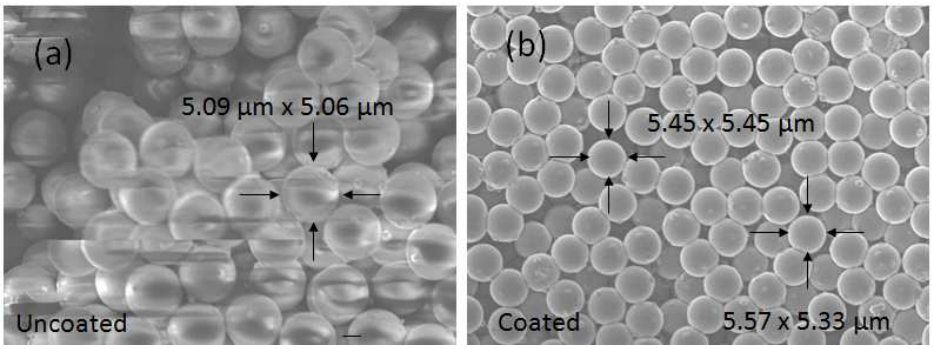

Figure 2.17. SEM images of uncoated and coated 5 µm silica microspheres.
3000× magnification (scale bar = 1 µm) and (b) 1600× magnification (scale bar = 10 µm). (a) uncoated silica microspheres at 3000x magnification and (b) silica microspheres coated with pHEMA at 1500x magnification. Scale bars represent 10 µm.

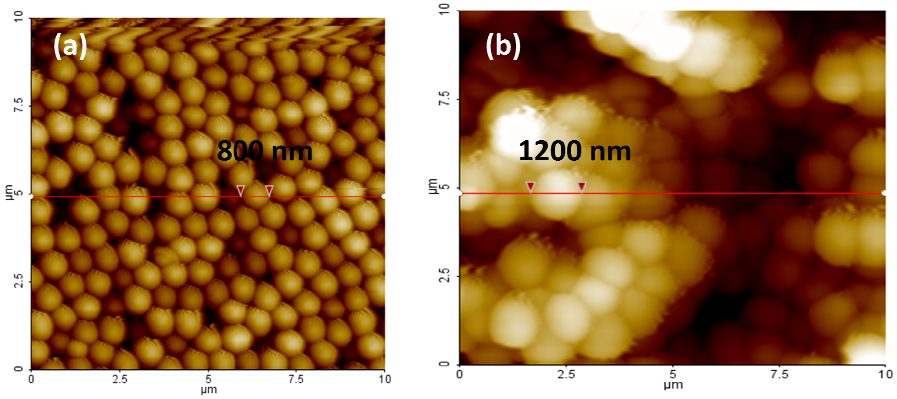

Figure 2.18. AFM images of uncoated and coated 800 nm silica microspheres.
(a) uncoated 800 nm silica spheres and (b) coated silica spheres. Both images were obtained with non contact method.